Inorg. Chem. **2006**, *45*, 521–528

Probing the Vanadyl and Molybdenyl Bonds in Complex Vanadomolybdate Structures

Jared P. Smit,[§] Hack-Sung Kim,[§] Jason D. Pless, Peter C. Stair,* and Kenneth R. Poeppelmeier*

Department of Chemistry, Northwestern University, Evanston, Illinois 60208

Received October 7, 2005

A solid solution was found to exist in the quaternary Li_2O–MgO–V_2O_5–MoO_3 system between the two phases $Mg_{2.5}VMoO_8$ and $Li_2Mg_2(MoO_4)_3$. Both $Mg_{2.5}VMoO_8$ and $Li_2Mg_2(MoO_4)_3$ are isostructural with the mineral lyonsite, and substitution according to the formula $\square_{1/4-x/6}Li_{4x/3}Mg_{15/4-7x/6}V_{3/2-x}Mo_{3/2+x}O_{12}$ ($0 \leq x \leq 1.5$, where $\square$ denotes a cation vacancy) demonstrates that a complete solid solution exits coupling the addition of molybdenum and lithium with the subtraction of cation vacancies, magnesium, and vanadium and vice versa. Vibrational Raman spectroscopy indicates that molybdenum–oxo double bonds preferentially associate with the cation vacancies.

Introduction

Lyonsite, α-$Cu_3Fe_4(VO_4)_6$,[1] is a naturally occurring mineral with a remarkable structure. The structure is ubiquitous in multicomponent vanadates and molybdates that form discreet V/MoO_4 tetrahedra, and various homeotypes have been studied for their properties ranging from ionic conduction to catalysis.[2,3] Numerous mixed-metal vanadates, molybdates, and tungstates adopt the lyonsite structure including $Li_3M(MoO_4)_3$ (M = Fe, Al, Ga, Cr, Sc, In),[3−6] $Li_2M_2(MoO_4)_3$ (M = Fe, Co, Ni, Mg, Mn, Zn),[7,8] $Li_2Zr(MoO_4)_3$,[9] $NaCo_{2.31}(MoO_4)_3$,[10] $Cu_{3.85}(MoO_4)_3$,[11] $Na_{2-2x}M_{2+x}(MoO_4)_3$ (M = Mg, Zn, Co, and Cu),[7,12] $M_{2.5}VMoO_8$ (M = Mg, Zn, Mn, Co),[13−16] $Mg_{2.5}VWO_8$,[17] $Li_2Mg_2(WO_4)_3$,[18] $Co_4Fe_{3.33}(VO_4)_6$,[19] $Co_{3.6}Fe_{3.6}(VO_4)_6$,[20] $Co_5Cr_{2.667}(VO_4)_6$,[21] $Cu_{4.05}Cr_{3.3}(VO_4)_6$,[22] and $Cu_4Fe_{3.33}(VO_4)_6$.[22]

The nominal lyonsite structure is orthorhombic (space group *Pnma*) and consists of V/Mo/W-centered tetrahedra linking zigzag sheets and columns formed by MO_6 octahedra and trigonal prisms (Figure 1). These isolated V/Mo/W-centered tetrahedra are joined to the inner wall of hexagonal tunnels formed by MO_6 octahedra and MO_6 trigonal prisms. Infinite columns of face-sharing MO_6 octahedra pass through the center of the tunnels (Figure 2a).

A striking feature of this structure is that it can incorporate a variable number of cationic vacancies for charge balance in order to accommodate numerous combinations of cations with different charges. For example, in $M_{2.5}VMoO_8$, one-sixteenth of the M (M = Mg, Zn, Mn, Co) sites are vacant. In $Co_{3.6}Cr_{3.6}(VO_4)_6$, one-tenth of the Co/Cr sites are vacant,

* To whom correspondence should be addressed. E-mail: krp@northwestern.edu (K.R.P.); pstair@northwestern.edu (P.C.S.).

§ Authors with equal contributions.

(1) Hughes, J. M.; Starkey, S. J.; Malinconico, M. L.; Malinconico, L. L. *Am. Mineral.* **1987**, *72*, 1000−1005.
(2) Harding, W. D.; Kung, H. H.; Kozhevnikov, V. L.; Poeppelmeier, K. R. *J. Catal.* **1993**, *144*, 597−610.
(3) Sebastian, L.; Piffard, Y.; Shukla, A. K.; Taulelle, F.; Gopalakrishnan, J. *J. Mater. Chem.* **2003**, *13*, 1797−1802.
(4) Klevtsov, P. V. *Kristallografiya* **1970**, *15*, 797−802.
(5) Trunov, V. K.; Efremov, V. A. *Zh. Neorg. Khim.* **1971**, *16*, 2026−2027.
(6) Kolitsch, U.; Tillmanns, E. *Acta Crystallogr., Sect. E* **2003**, *E59*, i55−i58.
(7) Efremov, V. A.; Trunov, V. K. *Zh. Neorg. Khim.* **1972**, *17*, 2034−2039.
(8) Penkova, V. G.; Klevtsov, P. V. *Zh. Neorg. Khim.* **1977**, *22*, 1713−1715.
(9) Klevtsova, R. F.; Antonova, A. A.; Glinskaya, L. A. *Kristallografiya* **1979**, *24*, 1043−1047.
(10) Ibers, J. A.; Smith, G. W. *Acta Crystallogr.* **1964**, *17*, 190−197.
(11) Katz, L.; Kasenally, A.; Kihlborg, L. *Acta Crystallogr., Sect. B* **1971**, *27*, 2071−2077.
(12) Efremov, V. A.; Trunov, V. K. *Izv. Akad. Nauk SSSR, Neorg. Mater.* **1975**, *11*, 273−277.
(13) Wang, X.; Stern, C. L.; Poeppelmeier, K. R. *J. Alloys Compd.* **1996**, *243*, 51−58.
(14) Wang, X.; Heier, K. R.; Stern, C. L.; Poeppelmeier, K. R. *J. Alloys Compd.* **1997**, *255*, 190−194.
(15) Wang, X.; Heier, K. R.; Stern, C. L.; Poeppelmeier, K. R. *J. Alloys Compd.* **1998**, *267*, 79−85.
(16) Kurzawa, M.; Bosacka, M.; Jakubus, P. *J. Mater. Sci.* **2003**, *38*, 3137−3142.
(17) Pless, J. D.; Kim, H.-S.; Smit, J. P.; Wang, X.; Stair, P. C.; Poeppelmeier, K. R. *Inorg. Chem.* **2005**, in press.
(18) Fu, Z.; Li, W. *Powder Diffr.* **1994**, *9*, 158−160.
(19) Wang, X.; Vander Griend, D. A.; Stern, C. L.; Poeppelmeier, K. R. *Inorg. Chem.* **2000**, *39*, 136−140.
(20) Belik, A. A.; Izumi, F.; Ikeda, T.; Nisawa, A.; Kamiyama, T.; Oikawa, K. *Solid State Sci.* **2002**, *4*, 515−522.
(21) Malakho, A. P.; Belik, A. A.; Lazoryak, B. I. *Zh. Neorg. Khim.* **2003**, *48*, 709−714.
(22) Belik, A. A.; Malakho, A. P.; Pokholok, K. V.; Lazoryak, B. I. *J. Solid State Chem.* **2001**, *156*, 339−348.

10.1021/ic051741+ CCC: $33.50
Published on Web 12/27/2005

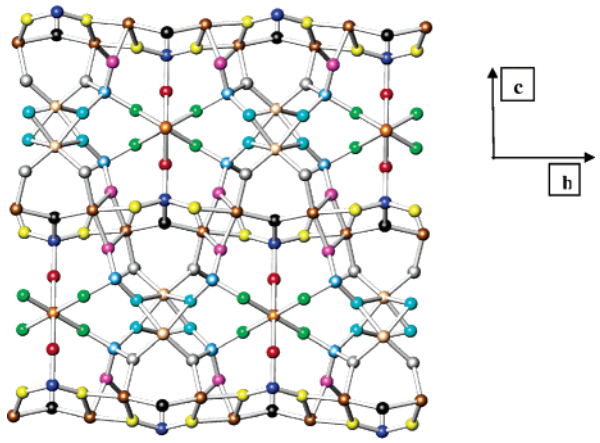

Figure 1. Structure of $Mg_{2.5}VMoO_8/Li_2Mg_2(MoO_4)_3$. Mo/V(1), dark blue; Mo/V(2), light blue; Mg/Li(1), dark orange; Mg/Li(2), orange (in the middle of the pseudo-hexagonal tunnel); Mg/Li(3), light orange; O(1), gray; O(2), red; O(3), yellow; O(4), black; O(5), green; O(6), pink; O(7), turquoise.

and in naturally occurring lyonsite, α-$Cu_3Fe_4(VO_4)_6$, a full one-eighth of the Cu/Fe sites are not occupied. In contrast, although cation vacancies are common, many of the molybdate phases, such as $Li_2M_2(MoO_4)_3$ (M = Fe, Co, Ni, Mg, Mn, Zn) and $Li_3M(MoO_4)_3$ (M = Fe, Al, Ga, Cr, Sc, In), have no vacancies associated with the Li/M site. However, vacancies can be created in these molybdates, for example, by replacing lithium with magnesium $Li_{2-2x}Mg_{2+x}(MoO_4)_3$ ($0 \le x \le 0.3$).[3]

While most of the known lyonsite-type molybdates have no associated cation vacancies, all of the known lyonsite-type vanadates have associated cation vacancies. Thus, while a large number of quaternary molybdates crystallize in the lyonsite structure, it is much less common for vanadates. Instead, many mixed-metal vanadates avoid cation vacancies and adopt either the triclinic β-$Cu_3Fe_4(VO_4)_6$[23] or the triclinic $GaZn_2V_3O_{11}$[24] structure types. When cation vacancies are present in the lyonsite structure, the vacancies are localized within the infinite chains of face-sharing MO_6 octahedra (Figure 2a) in order to minimize the Coulombic repulsions associated with the close positioning of cations at the center of these face-sharing octahedra.[25]

In addition to, and in part a result of, the large concentration of cation vacancies that can be incorporated, the lyonsite structure can accommodate a wide variety of metals. A large number of mono-, di-, tri-, and tetravalent metals have each been shown to occupy the MO_6 octahedral and trigonal prismatic positions, while only three metals, vanadium (V^{5+}), molybdenum (Mo^{6+}), and tungsten (W^{6+}), are known to occupy the tetrahedral positions. With this in mind, there exists the general possibility to form various solid solutions by coupling the substitution of M^+, M^{2+}, M^{3+}, or M^{4+} among themselves with charge balance achieved by a combination of cation vacancies and the substitution of M^{5+} for M^{6+}, or vice versa, in the tetrahedral positions.

To demonstrate this phenomenon, $Mg_{2.5}VMoO_8$ and $Li_2Mg_2(MoO_4)_3$ were chosen to form a solid solution according to the formula $\square_{1/4-x/6}Li_{4x/3}Mg_{15/4-7x/6}V_{3/2-x}Mo_{3/2+x}O_{12}$ ($0 \le x \le 1.5$, where $\square$ denotes a cation vacancy). The formula is remarkably complex but can be described simply by one variable. More specifically, lithium (Li^+) was substituted for magnesium (Mg^{2+}) in $Mg_{2.5}VMoO_8$, and charge neutrality was maintained by the simultaneous substitution of molybdenum (Mo^{6+}) for vanadium (V^{5+}), concurrent with a reduction in the number of cation vacancies.

Both $Mg_{2.5}VMoO_8$ and $Li_2Mg_2(MoO_4)_3$ have interesting properties. The surface of $Mg_{2.5}VMoO_8$ has been shown to effectively catalyze the oxidative dehydrogenation of propane and butane.[2,26] Recently, $Mg_{2.5}VMoO_8$ has been used as a photocatalyst for O_2 evolution under visible light,[27] while $Li_2Mg_2(MoO_4)_3$ is part of the NASICON family, which are well known for their conductive properties.[3] A solid solution between the compounds is interesting because the addition of alkali metals to oxidation catalysts often reduces the acidity and improves selectivity. Additionally, the creation of cationic vacancies in ionic conductors is advantageous because it facilitates lithium mobility. This work illustrates the remarkable function of cation vacancies to preserve solid-state structures, which can lead to new and significant solid-state chemistry.

The structures of various bulk and supported metal oxides (e.g., vanadates, molybdates, and tungstates) have been characterized extensively by Raman spectroscopy.[28,29] Raman spectroscopy is sensitive to oxidation states and the short-range coordination environment around metal and oxygen ions and is particularly useful in operando[30] or in-situ studies for surface species where crystallinity and homogeneity are in question. Raman spectra of surface species are frequently ambiguous and difficult to assign clearly. For example, higher-order metal−oxo bonds on the surface of metal oxides have been identified by comparing observed Raman frequencies with the nominal M=O frequency range. Primarily, the ambiguity results from the overlap of the nominal M=O stretching region, ~900−1040 cm^{-1},[31] with the ν_1 stretching frequency region for MO_x polyhedra (e.g., ν_1 band for WO_4 tetrahedra with T_d symmetry appears at 931 cm^{-1}). Also, the vibrational frequency of the M=O stretching depends on the local environments of the metal and oxygen, as well as the metal type and the oxidation state of the metal, i.e., the coordination number of the metal, the degree of angular distortion of the MO_x polyhedra, M−O bond length, and the coordination of other chemical species (cations) to the oxygen.[31,32] The detailed structural information such as

(23) Lafontaine, M. A.; Greneche, J. M.; Laligant, Y.; Ferey, G. *J. Solid State Chem.* **1994**, *108*, 1−10.
(24) Mueller, C.; Mueller-Buschbaum, H. *J. Alloys Compd.* **1993**, *191*, 251−253.
(25) Wang, X.; Pless, J. D.; Griend, D. A. V.; Stair, P. C.; Poeppelmeier, K. R.; Hu, Z.; Jorgensen, J. D. *J. Alloys Compd.* **2004**, *379*, 87−94.
(26) Pless, J. D.; Bardin, B. B.; Kim, H.-S.; Ko, D.; Smith, M. T.; Hammond, R. R.; Stair, P. C.; Poeppelmeier, K. R. *J. Catal.* **2004**, *223*, 419−431.
(27) Wang, D.; Zou, Z.; Ye, J. *Catal. Today* **2004**, *93*−*95*, 891−894.
(28) Nakamoto, K. *Infrared and Raman Spectra of Inorganic and Coordination Compounds, Part A: Theory and Applications in Inorganic Chemistry*, 5th ed.; John Wiley: New York, 1997.
(29) Stencel, J. M. *Raman Spectroscopy for Catalysis*; Van Nostrand Reinhold: New York, 1990.
(30) Guerrero-Perez, M. O.; Banares, M. A. *Chem. Commun. (Cambridge)* **2002**, 1292−1293.
(31) Banares, M. A.; Wachs, I. E. *J. Raman Spectrosc.* **2002**, *33*, 359−380.

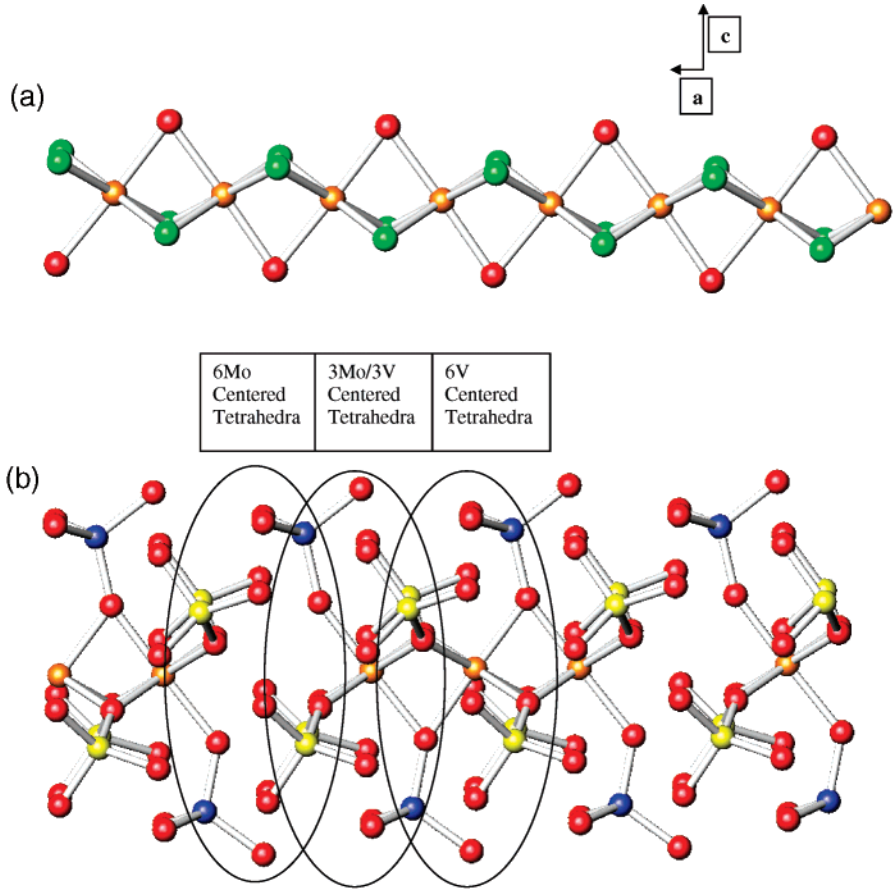

Figure 2. (a) Face-sharing octahedra. Mg/Li(2), orange; O(2), red; O(5), green. (b) Face-sharing octahedra surrounded by six MoO_4 around the vacancy (left oval) and six VO_4 tetrahedra around the middle Mg of a Mg trimer (right oval). The V/Mo(1) position is blue, and the V/Mo(2) position is yellow.

coordination geometry, bond lengths, and bond angles that can be obtained by single-crystal X-ray crystallography[17] or X-ray absorption spectroscopy[33] combined with vibrational spectroscopic data can provide additional insight and more reliable vibrational assignments.

In a companion paper, high-frequency Mo═O stretching vibrations were associated with cation vacancies.[17] In this work, the assignments are further supported by the $Li_2Mg_2(MoO_4)_3-Mg_{2.5}VMoO_8$ solid solution, wherein lower concentrations of cation vacancies correlate with a systematic decrease in the oxygen pπ−molybdenum dπ bonding. In addition, because there is no definitive evidence for a V═O double bond, local ordering that places primarily MoO_4 tetrahedra around the cation vacancies is discussed.

Experimental Section

Compounds were synthesized by the stoichiometric addition of Li_2CO_3 (Aldrich, 99+%), MgO (Alfa Aesar, 99.95%), V_2O_5 (Alfa Aesar, 99.6%), and MoO_3 (Alfa Aesar, 99.95%). Powders were heated in platinum crucibles at 850−1000 °C.

Powder X-ray diffraction (PXRD) data for the refinements were collected every 0.01° for $10° < 2\theta < 70°$ on a Scintag XDS 2000 diffractometer with Ni-filtered Cu Kα radiation ($\lambda = 1.5418$ Å) with 1 s per step. Lattice parameters were refined using EXPGUI graphical interface for GSAS[34] with the structural parameters of $Mg_{2.5}VMoO_8$[35] and $Li_2Mg_2(MoO_4)_3$[3] as a starting reference.

Unpolarized Raman spectra (100−1200 cm^{-1}) of the polycrystalline samples were collected on a Bio-Rad FT-Raman spectrophotometer with 0.5 cm^{-1} resolution and 200 scans.

Results and Discussion

Formation of the Solid Solution of $\square_{1/4-x/6}Li_{4x/3}Mg_{15/4-7x/6}V_{3/2-x}Mo_{3/2+x}O_{12}$ ($0 \le x \le 1.5$). Limited solid solutions of $Mg_{2.5}VMoO_8$ with differing amounts of Mg, V, and Mo have been reported previously.[13,25] The concentration of cation vacancies varies with the vanadium and molybdenum concentrations according to the formula $Mg_{2.5+x}V_{1+2x}Mo_{1-2x}O_8$ ($-0.05 \le x \le 0.05$).[25] At the same time, the charge is balanced by a corresponding gain or loss of Mg^{2+} ions. Recently, a solid solution has been reported for $Li_2Mg_2(MoO_4)_3$ as $Li_{2-2x}Mg_{2+x}(MoO_4)_3$ ($0 \le x \le 0.3$), which also results in cation vacancies.[3] Owing to the previously reported versatility of the structure with regards to cation vacancies and solid solutions, the solid solution should exist between $Mg_{2.5}VMoO_8$ and $Li_2Mg_2(MoO_4)_3$.

Both $Mg_{2.5}VMoO_8$ and $Li_2Mg_2(MoO_4)_3$ adopt the same lyonsite-type structure consisting of vanadium or molybdenum tetrahedra linking zigzag sheets and columns formed

(32) Busca, G. *J. Raman Spectrosc.* **2002**, *33*, 348−358.
(33) Kim, H.-S.; Pasten, P. A.; Gaillard, J.-F.; Stair, P. C. *J. Am. Chem. Soc.* **2003**, *125*, 14284−14285.
(34) Toby, B. H. *J. Appl. Crystallogr.* **2001**, *34*, 210−213.
(35) Zubkov, V. G.; Leonidov, I. A.; Poeppelmeier, K. R.; Kozhevnikov, V. L. *J. Solid State Chem.* **1994**, *111*, 197−201.

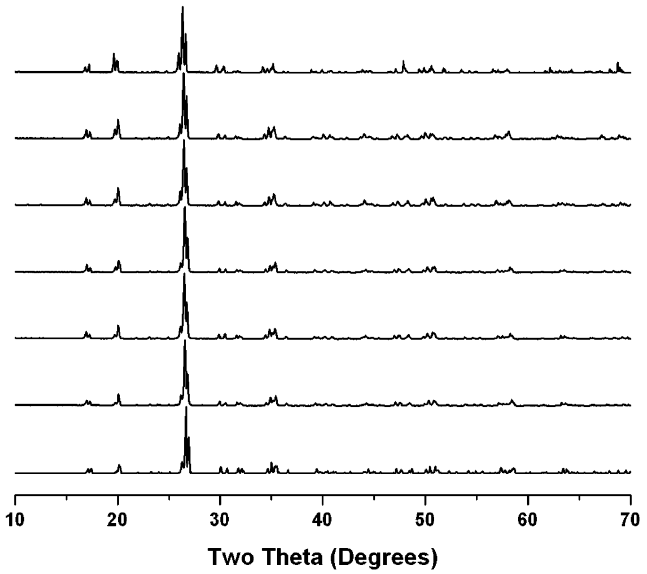

Figure 3. Powder X-ray diffraction patterns. $Mg_{2.5}VMoO_8$ ($x = 0$), bottom; $x = 0.25$, 2nd from bottom; $x = 0.50$, 3rd from bottom; $x = 0.75$, 4th from bottom; $x = 1.00$, 5th from bottom; $x = 1.25$, 6th from bottom; $Li_2Mg_2(MoO_4)_3$ ($x = 1.5$), top.

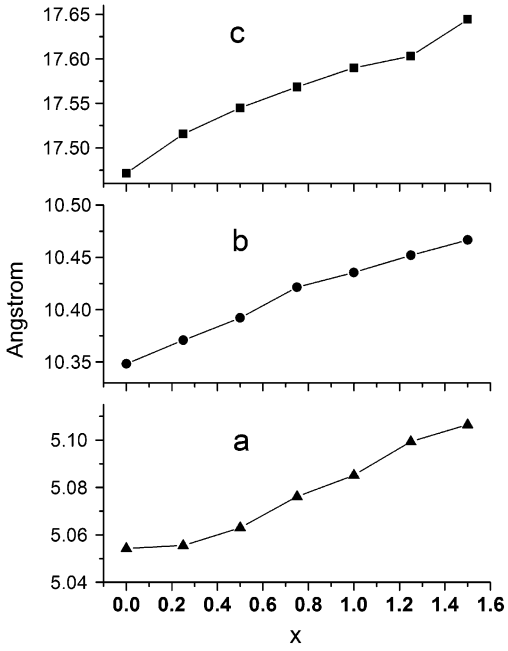

Figure 4. Variation of unit cell parameters *a*, *b*, and *c* as a function of *x* in the formula $\square_{1/4-x/6}Li_{4x/3}Mg_{15/4-7x/6}V_{3/2-x}Mo_{3/2+x}O_{12}$ ($0 \le x \le 1.5$).

by lithium or magnesium octahedra and trigonal prisms, as previously described. It is possible to understand how the formulas are related by considering cation vacancies. $Mg_{2.5}VMoO_8$, with $Z = 6$, can be written as $Mg_{15}V_6Mo_6O_{48}$. Magnesium cations occupy three crystallographically distinct positions: an 8d, and two separate 4c positions, for a total of 16 magnesium positions. Therefore, one-sixteenth of the Mg positions are vacant, and $Mg_{2.5}VMoO_8$ can be rewritten as $\square_{1/6}Mg_{2.5}VMoO_8$ or $\square_{1/4}Mg_{15/4}V_{3/2}Mo_{3/2}O_{12}$.

Further inspection of the end member formulations revealed that it is easier to determine the substitution pattern of lithium into $Mg_{2.5}VMoO_8$ when the formulations are normalized with the same oxygen stoichiometry as $\square_{1/4}Mg_{15/4}V_{3/2}Mo_{3/2}O_{12}$ and $Li_2Mg_2Mo_3O_{12}$. A more general formula can be written as $A_4B_3O_{12}$, where A = some combination of $\square$, Li, or Mg, and B = some combination of V or Mo. On the basis of these observations, the formula $\square_{1/4-x/6}Li_{4x/3}Mg_{15/4-7x/6}V_{3/2-x}Mo_{3/2+x}O_{12}$ ($0 \le x \le 1.5$) was derived.

Substitution according to the formula $\square_{1/4-x/6}Li_{4x/3}Mg_{15/4-7x/6}V_{3/2-x}Mo_{3/2+x}O_{12}$ ($0 \le x \le 1.5$) was successful. X-ray diffraction shows no evidence of other phases (Figure 3). Additionally, a lattice shift is observed as *x* increases. The peaks shift to a lower angle, indicating a larger *d*-spacing, which is expected owing to the slightly larger size of lithium and molybdenum.

The unit cell for $Mg_{2.5}VMoO_8$ has been determined to be $a = 5.0543(2)$ Å, $b = 10.3483(4)$ Å, and $c = 17.4713(7)$ Å and is in good agreement with the published values $a = 5.0515(1)$ Å, $b = 10.3455(2)$ Å, $c = 17.4683(4)$ Å from PXRD.[35] Likewise, the unit cell for $Li_2Mg_2(MoO_4)_3$ has been determined to be $a = 5.1064(7)$ Å, $b = 10.4666(14)$ Å, and $c = 17.6443(23)$ Å. The published values for $Li_2Mg_2(MoO_4)_3$ are $a = 5.1167(2)$ Å, $b = 10.4646(4)$ Å, and $c = 17.6228(8)$ Å from single-crystal X-ray diffraction.[3] Owing to the slightly larger sizes of both lithium and molybdenum compared to magnesium and vanadium respectively, the lattice constants of $Li_2Mg_2(MoO_4)_3$ are noticeably larger when compared to those of $Mg_{2.5}VMoO_8$.

The unit cell parameters and volume obtained for compounds corresponding to $x = 0$, 0.25, 0.50, 0.75, 1.00, 1.25, and 1.5 for the formula $\square_{1/4-x/6}Li_{4x/3}Mg_{15/4-7x/6}V_{3/2-x}Mo_{3/2+x}O_{12}$ ($0 \le x \le 1.5$) are listed in Table 1. The lattice parameters increase as more lithium and molybdenum are incorporated and magnesium and vanadium are removed, corresponding to the aforementioned shift in peaks to lower 2θ. Graphs displaying the increasing lattice parameters as a function of *x* are shown in Figure 4, and Figure 5 displays the increase in volume as a function of *x*.

Initial attempts at forming the solid solution based on the formula $Li_xMg_{2.5-x}V_{1-x}Mo_{1+x}O_8$ failed and resulted in the formation of a mixture of the phases $Li_2Mg_2(MoO_4)_3$ and $MgMoO_4$ when $x = 1$. This is expected as the lithium-rich end member would be '$LiMg_{1.5}Mo_2O_8$' or '$Li_2Mg_3Mo_4O_{16}$',

Table 1. Unit Cell Parameters and Volume for $\square_{1/4-x/6}Li_{4x/3}Mg_{15/4-7x/6}V_{3/2-x}Mo_{3/2+x}O_{12}$ ($0 \le x \le 1.5$)

x	formulation	*a* (Å)	*b* (Å)	*c* (Å)	*V* (Å^3)
0	$Mg_{2.5}VMoO_8$	5.0543(2)	10.3483(4)	17.4713(7)	913.81(6)
0.25	$\square_{0.21}Li_{0.33}Mg_{3.46}V_{1.25}Mo_{1.75}O_{12}$	5.0555(4)	10.3707(6)	17.5156(12)	918.33(29)
0.50	$\square_{0.17}Li_{0.67}Mg_{3.17}V_{1.00}Mo_{2.00}O_{12}$	5.0630(4)	10.3921(7)	17.5448(12)	923.12(34)
0.75	$\square_{0.13}Li_{1.00}Mg_{2.86}V_{0.75}Mo_{2.25}O_{12}$	5.0761(5)	10.4213(8)	17.5684(2)	929.36(8)
1.00	$\square_{0.08}Li_{1.33}Mg_{2.58}V_{0.50}Mo_{2.50}O_{12}$	5.0851(9)	10.4355(16)	17.5899(27)	933.42(389)
1.25	$\square_{0.04}Li_{1.67}Mg_{2.29}V_{0.25}Mo_{2.75}O_{12}$	5.0993(3)	10.4519(5)	17.6030(8)	938.19(12)
1.50	$Li_2Mg_2(MoO_4)_3$	5.1064(7)	10.4666(14)	17.6443(23)	943.03(225)

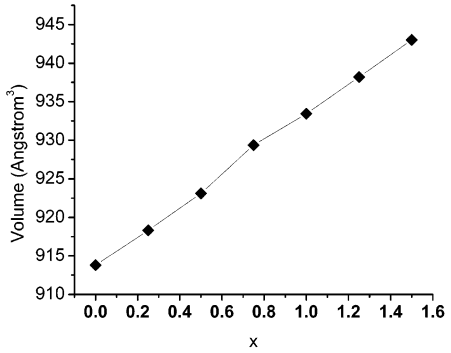

Figure 5. Variation of unit cell volume as a function of x in the formula $\square_{1/4-x/6}Li_{4x/3}Mg_{15/4-7x/6}V_{3/2-x}Mo_{3/2+x}O_{12}$ ($0 \le x \le 1.5$).

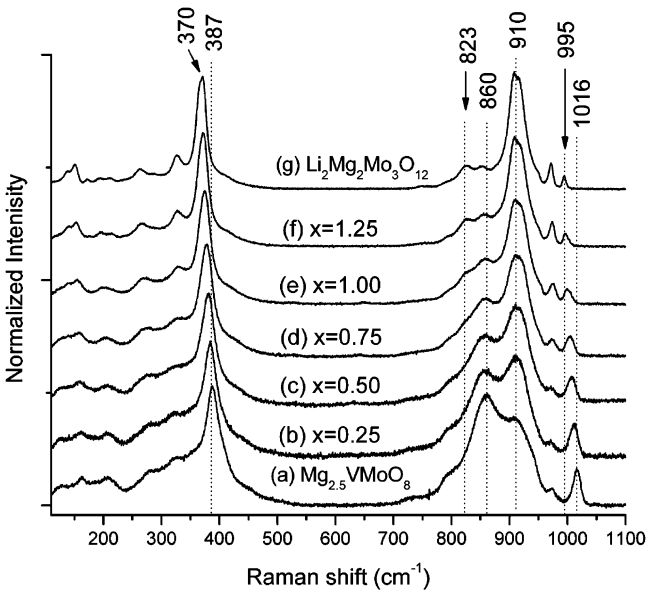

Figure 6. Raman spectra of the solid solution $\square_{1/4-x/6}Li_{4x/3}Mg_{15/4-7x/6}V_{3/2-x}Mo_{3/2+x}O_{12}$ ($0 \le x \le 1.5$). Intensities are normalized to a strong band attributed to the bending vibration centered at 370−387 cm^{-1}.

which is not a known compound. The end member of the solid solution is $Li_2Mg_2Mo_3O_{12}$.

In contrast to solid solutions where one or two metals and the ratio therein is varied, changing x in the formula $\square_{1/4-x/6}Li_{4x/3}Mg_{15/4-7x/6}V_{3/2-x}Mo_{3/2+x}O_{12}$ ($0 \le x \le 1.5$) affects the stoichiometry of four metals and corresponding vacancies in order to maintain compositions where one phase is observed. The solid-state crystal chemistry with other combinations of metal oxides that can be envisioned with only one variable in solid solutions that parallel $\square_{1/4-x/6}Li_{4x/3}Mg_{15/4-7x/6}V_{3/2-x}Mo_{3/2+x}O_{12}$ ($0 \le x \le 1.5$) appears to be extensive.

Raman Spectra of the Solid Solution. Figure 6 displays the Raman spectra for the solid solution of $\square_{1/4-x/6}Li_{4x/3}Mg_{15/4-7x/6}V_{3/2-x}Mo_{3/2+x}O_{12}$ ($0 \le x \le 1.5$) at formulations corresponding to $x = 0.25$, 0.50, 0.75, 1.00, 1.25, as well as the end members $Mg_{2.5}VMoO_8$ (when $x = 0$) and $Li_2Mg_2(MoO_4)_3$ (when $x = 1.5$). On the basis of known trends of positions and relative intensities of the ν_1-(A_1) Raman bands for VO_4, MoO_4, and WO_4 tetrahedra and by comparing Raman spectral features for $Mg_{2.5}VMoO_8$ and $Mg_{2.5}VWO_8$ in a companion paper,[17] the bands centered at 910 and 860 cm^{-1} in the Raman spectrum of $Mg_{2.5}VMoO_8$ are assigned to the symmetric stretching ν_1 mode of MoO_4 and VO_4 tetrahedra, respectively. The bands at 370 and 387 cm^{-1} are assigned to the bending ($\nu_2(E)$ or $\nu_4(T_2)$) vibration of MoO_4 and VO_4 tetrahedra, respectively. Also, bands at 823 and 791 cm^{-1} are assigned to $\nu_3(T_2)$ asymmetric stretching vibration of MoO_4 and VO_4 tetrahedra, respectively. The intensity of the bands varies with the content of vanadium (See Tables 1 and 2, and Figure 6), which strongly supports these assignments. The ν_2 band positions of the aqueous MoO_4^{2-} and VO_4^{3-} tetrahedra have been observed at 317 and 336 cm^{-1}, respectively, and are estimated to overlap with the ν_4 band positions.[28] A relatively weak, but distinct band (see Figure 6d−g) at 326 cm^{-1} is likely due to the $\nu_2(E)$ or $\nu_4(T_2)$ bending vibration of MoO_4 tetrahedra because it is stronger when the Mo concentration is relatively higher.

M═O Stretching Vibrations. M═O (M = V, Mo, W, etc.) stretching Raman bands generally appear at ∼900−1040 cm^{-1}.[36] While the high-frequency metal−oxo bands observed in Figure 6 are of similar frequency to surface M═O species, it is important to note that none of the oxygen atoms are likely to be singly coordinated. Each oxygen atom is three coordinate in $Li_2Mg_2Mo_3O_{12}$, when no cation vacancies are present. However, as vacancies are incorporated at the Li/Mg(2) position, the coordination environments of O(2) and O(5) are changed. Instead of bonding to two Li/Mg(2) and one V/Mo(1) or V/Mo(2) (three total bonds), O(2) and O(5) are bonded to only one Li/Mg(2) and one V/Mo(1) or V/Mo(2) (two total bonds), respectively. The double-bond character that is reflected in the high-frequency Raman bands is a result of the two-coordinate oxygen atoms being more strongly bonded to the higher-valent transition metal ion.

In a companion paper, the Raman spectrum for isostructural $Mg_{2.5}VWO_8$ showed a band at 1035 cm^{-1}, which was assigned to the W═O stretching vibration, and showed no other bands in the ∼970−1030 cm^{-1} range.[17] Because vanadium is common to both $Mg_{2.5}VMoO_8$ and $Mg_{2.5}VWO_8$, V═O-related vibrations are expected to appear at the same frequency in the vibrational spectra for the respective materials. Therefore, the Raman bands observed at ∼970−1016 cm^{-1} in Figure 6 should be attributed to MoO-related, and not VO-related, vibrations. The band centered at 1016 cm^{-1} in the Raman spectrum of $Mg_{2.5}VMoO_8$ was assigned to the Mo═O stretching vibration of the molybdenum−oxo bond located next to Mg(2) cation vacancies.[17] The Raman spectrum of $Li_2Mg_2(MoO_4)_3$ does not show the band at 1016 cm^{-1} (Figure 6g), which strongly supports the assignment because $Li_2Mg_2(MoO_4)_3$ does not contain vacancies. Additionally, the band position at 1016 cm^{-1} matches well with surface terminal Mo═O stretching vibrations seen at 1012 cm^{-1}.[37] The relatively lower intensity of the band at 1016 than 910 cm^{-1} (the symmetric stretching ν_1 mode of MoO_4)

(36) Mestl, G.; Srinivasan, T. K. K. *Catal. Rev. − Sci. Eng.* **1998**, *40*, 451−570.
(37) Chan, S. S.; Wachs, I. E.; Murrell, L. L.; Wang, L.; Hall, W. K. *J. Phys. Chem.* **1984**, *88*, 5831−5835.

Table 2. Assignments and Raman Wavenumber Shifts in cm^{-1} of VO_4^{3-} and MoO_4^{2-} Tetrahedra in the Solid Solution[d]

Point group, symmetry species, vibrational mode (all modes are Raman active), and the correlation					$Mg_{2.5}VMoO_8$ (when x = 0)		$Li_2Mg_2(MoO_4)_3$ (when x = 1.50), & x = 0.25-1.50
T_d: 4 frequencies			C_S: 9 frequencies		MoO_4^{2-}	VO_4^{3-}	MoO_4^{2-}
ν_s(M-O)	ν_1, A_1	→	ν_s(M-O)	A'	910	860↓	910↑
		→	ν_s(M-O_s)[a]		1016 (Mo=O), 974 (Mo⋯O---Mg)	944 (V⋯O)	995-1012↑ (Mo⋯O---Li), 974↑ (Mo⋯O---Mg)
ν_{as}(M-O)	ν_3, T_2	→	ν_s(M-O_l)[a]		807[b]	799[b]	853[c]
			MO_2 scissor		370,	387↓	370↑
			MO_2 wag		326		326↑
Bending (O-M-O)	ν_2, E		Deformation				
	ν_4, T_2		MO_2 rock	A''			
			MO_2 twist				
		→	ν_{as}(M-O)		823	791↓	823↑

[a] O_s and O_l is the oxygen with a shorter and a longer M−O bond length, respectively, than any others. M = V, Mo. [b] Estimated for the V/Mo−O bond length of 1.77 Å. [c] Estimated for the Mo−O bond length of 1.79 Å. [d] ↑ and ↓ means that the band is stronger and weaker, respectively, as x increases from 0 to 1.5. The MoO_4^{2-} column on the left refers only to $Mg_{2.5}VMoO_8$, while the MoO_4^{2-} column on the right refers to the phases corresponding from x = 0.25 to x = 1.50. The VO_4^{3-} column in the middle is common to the phases from x = 0 to x = 1.25.

in the Raman spectrum of $Mg_{2.5}VMoO_8$ (Figure 6a) can be explained by the low concentration of the vacancies (6.25%).

The band centered at 1016 cm^{-1} in the Raman spectrum of $Mg_{2.5}VMoO_8$ (x = 0) seen in Figure 6a gradually shifts to lower wavenumbers, and the intensity becomes weaker as x in the formula $\square_{1/4-x/6}Li_{4x/3}Mg_{15/4-7x/6}V_{3/2-x}Mo_{3/2+x}O_{12}$ ($0 \le x \le 1.5$) increases. The gradual red-shifts and the weakening of the shifted bands as x increases from 0 to 1.50 are likely due to a systematic decrease in the oxygen pπ−molybdenum dπ bonding related to the decrease in the number of the Mg(2) cation vacancies. The weaker bonds are reflected in the increase of the average bond lengths of Mo(1)−O(2) and Mo(2)−O(5) and the expansion of the unit cell dimensions (see Tables 1 and 3).

Structural distortion of the tetrahedral MO_4 ion that lowers the T_d symmetry to C_S symmetry was discussed in a companion paper[17] and the band at 974 cm^{-1} seen in Figure 6a was assigned to the symmetric stretching (A' symmetry, C_S group) vibration of Mo═O-type (i.e., Mo⋯O) bonds where Mg^{2+} binds to the oxygen. This assignment is supported by the appearance of the band at ∼974 cm^{-1} in the Raman spectra for all compositions of the solid solution because Mg^{2+} is common to each phase and by the absence of the band in the Raman spectrum of $Mg_{2.5}VWO_8$, where the Mo is replaced by W.[17] The band position is in good agreement with a band observed at 967 cm^{-1} from the Mo−O stretching in the distorted MoO_4 tetrahedra of $MgMoO_4$.[38] The shortest Mo−O bond length in $MgMoO_4$ is 1.73 Å,[39] while the shortest Mo−O bond length in $Li_2Mg_2(MoO_4)_3$, 1.745 Å for Mo(1)−O(2) (see Table 3), is similar to that observed for $MgMoO_4$. The Mo−O bond order in Mo⋯O- - -Mg^{2+} for a frequency of 971−974 cm^{-1} is estimated to be ∼1.8.[38]

Table 3. Comparison of Bond Lengths Reproduced from Refs 3 and 13 for All the Atoms that Are on the Same Positions in Isostructural $Li_2Mg_2Mo_3O_{12}$ and $Mg_{2.5}VMoO_8$[a]

$Mg_{2.5}VMoO_8$ (x = 0)		$Li_2Mg_2Mo_3O_{12}$ (x = 1.5)	
V/Mo(1)−O(2)	1.713(4)	Mo(1)−O(2)	1.745(2)
V/Mo(1)−O(3) × 2	1.741(3) × 2	Mo(1)−O(3) × 2	1.765(2) × 2
V/Mo(1)−O(4)	1.770(5)	Mo(1)−O(4)	1.793(3)
V/Mo(2)−O(1)	1.758(3)	Mo(2)−O(1)	1.780(2)
V/Mo(2)−O(5)	1.716(3)	Mo(2)−O(5)	1.768(2)
V/Mo(2)−O(6)	1.745(3)	Mo(2)−O(6)	1.786(2)
V/Mo(2)−O(7)	1.744(3)	Mo(2)−O(7)	1.749(2)
Mg(1)−O(1)	2.038(3)	M(1)−O(1)	2.055(2)
Mg(1)−O(3)	2.071(4)	M(1)−O(3)	2.099(3)
Mg(1)−O(3)	2.142(4)	M(1)−O(3)	2.186(2)
Mg(1)−O(4)	2.066(3)	M(1)−O(4)	2.110(2)
Mg(1)−O(6)	2.072(4)	M(1)−O(6)	2.076(2)
Mg(1)−O(6)	2.095(4)	M(1)−O(6)	2.117(2)
Mg(2)−O(2) × 2	2.106(6), 2.119(6)	M(2)−O(2) × 2	2.129(4) × 2
Mg(2)−O(5) × 2	2.049(4) × 2	M(2)−O(5) × 2	2.050(3) × 2
Mg(2)−O(5) × 2	2.066(4) × 2	M(2)−O(5) × 2	2.058(3) × 2
Mg(3)−O(1) × 2	2.059(4) × 2	M(3)−O(1) × 2	2.133(3) × 2
Mg(3)−O(7) × 2	2.117(4) × 2	M(3)−O(7) × 2	2.172(4) × 2
Mg(3)−O(7) × 2	2.178(4) × 2	M(3)−O(7) × 2	2.206(3) × 2

[a] All of the atomic labels from ref 13 were converted to the numbering system used in ref 3 for clarity.

Similarly, the bands at 995−1012 cm^{-1} seen in Figure 6b−g are assigned to the symmetric stretching (A' symmetry, C_S group) vibration of Mo═O-type (i.e., Mo⋯O) bonds where Li^+ binds to the oxygen. The Li^+ coordination to the oxygen increases the Mo═O bond length, which

(38) Hardcastle, F. D.; Wachs, I. E. *J. Raman Spectrosc.* **1990**, *21*, 683−691.

(39) Bakakin, V. V.; Klevtsova, R. F.; Gaponenko, L. A. *Kristallografiya* **1982**, *27*, 38−42.

lowers the Mo═O stretching frequency. As x in the formula $\square_{1/4-x/6}Li_{4x/3}Mg_{15/4-7x/6}V_{3/2-x}Mo_{3/2+x}O_{12}$ ($0 \leq x \leq 1.5$) increases, the number of Li^+ bound to O(7) increases because it has been shown that the M(3) site is primarily occupied by Li^+ in $Li_2Mg_2Mo_3O_{12}$.[3] Additionally, the number of Li^+ bound to O(2) will increase as the M(2) cation vacancies are gradually filled. The gradual increase of Li^+ binding to O(2) and O(7) and subsequent decrease in π bonding between the oxygen p and molybdenum d orbitals are likely responsible for the red-shift of the Mo−O stretching frequency from 1016 to 995 cm^{-1}. This assignment is supported by the lack of the bands at 995−1012 cm^{-1} in the Raman spectrum of $Mg_{2.5}VMoO_8$ because it does not contain lithium.

Although tetrahedrally coordinated Li_2MoO_4 might be expected to be a model compound for estimating the stretching frequencies of Li^+-coordinated Mo−O (or Mo═O-type) bonds, the bond lengths and angles of Li_2MoO_4[40] are not a good match for modeling $Li_2Mg_2(MoO_4)_3$. The Mo−O bond lengths in $Li_2Mg_2(MoO_4)_3$ are shorter compared to the Mo−O bond lengths in Li_2MoO_4, and the MoO_4 tetrahedral angles in $Li_2Mg_2(MoO_4)_3$ show a greater degree of angular distortion compared to the MoO_4 tetrahedral angles in Li_2MoO_4[40] Therefore, the highest Mo−O Raman stretching frequency for $Li_2Mg_2(MoO_4)_3$ is estimated to appear at a higher frequency than the highest observed Mo−O stretching band at 903 cm^{-1} for the Li_2MoO_4.[41]

A more accurate model for Li^+ coordinated to Mo═O-type bonds may be the coordination of a hydrogen atom from a water molecule to the oxygen in terminal M═O bonds on surfaces. A band at 975 cm^{-1} has been attributed to surface terminal stretching vibrations of Mo═O where hydrogen in water is coordinated to the oxygen (i.e., Mo•••O- - -H in H_2O),[37] and is close in position to the observed band centered at 995 cm^{-1} in Figure 6. The Mo−O bond orders for the bands at 1016 and 995 cm^{-1} are estimated to be near 2.0 (i.e., ideal Mo═O double bond) and 1.9, respectively, from a correlation relating Mo−O bond order to Mo−O stretching frequency.[38]

Because MoO_3 is a strong Raman scatterer and was used as a starting material in the synthetic procedure, the two bands at 995 and 823 cm^{-1} appearing together in the Raman spectra of the $x = 1.0-1.5$ samples (Figure 6e−g) may be due to a trace amount of MoO_3. However, this possibility can be excluded owing to the lack of other characteristic strong bands of MoO_3[42] at 663 and 289 cm^{-1}, as well as the lack of any XRD diffraction peaks from MoO_3 and to the reproducible Raman spectra (i.e., appearance of the two bands at 995 and 823 cm^{-1}) when the samples were calcined at 900 °C, a temperature that is well above the melting point of MoO_3 (795 °C). The band at 823 cm^{-1} is assigned to the Mo−O asymmetric stretching vibration (see Table 2).

Since vanadium and molybdenum atoms equally occupy each V/Mo-centered tetrahedral position in the crystallographic model,[13] a Raman band attributed to the VO stretching vibration associated with the vacancies is expected to appear. The VO stretching vibration in the $Mg_{2.5}VMoO_8$ structure should appear above 1000 cm^{-1} since the terminal V═O stretching on surfaces typically appears in this region. However, the assignment of the band at 1016 cm^{-1} to V═O was excluded in the companion paper because a high-frequency band appeared only at 1035 cm^{-1} for $Mg_{2.5}VWO_8$, and the V═O vibration is expected to be located at the same frequency in these materials.[17]

The observed V/Mo(1)−O(2) bond length, which is dependent upon the crystallographic model, of 1.713 Å (see Table 3) should be an average of four bonds: The V(1)−O(2) that does not border a vacancy, the Mo(1)−O(2) that does not border a vacancy, the V(1)−O(2) that borders a vacancy, and the Mo(1)−O(2) that borders a vacancy. The bond lengths of the V(1)−O(2) and Mo(1)−O(2) bonds that border a vacancy are estimated to be ∼1.66 and ∼1.70 Å, respectively. The estimation is obtained from the average V/Mo(1)−O(2) crystallographic bond length of 1.713 Å, an estimated V/Mo(1)−O(2) bond length of ∼1.741 Å based on the V/Mo(1)−O(3) bond length that does not border a vacancy, as well as the degree of difference in V−O and Mo−O bond lengths in compounds[13] that are isostructural to $Mg_{2.5}VMoO_8$ but consist of ordered (i.e., V-only or Mo-only) tetrahedra. The estimated VO and MoO bond lengths of 1.66 and ∼1.70 Å correlate with a bond order of 1.5−1.6 and 1.8−2.0, respectively. This correlates with a vibrational frequency of 929 and 1016 cm^{-1}, respectively, on the basis of Wachs' correlation[43] and a correction for the degree of tetrahedral angular distortion assuming that the $Mo(1)O_4$ and $V(1)O_4$ tetrahedra have the same degree of tetrahedral angular distortion.

Recently, combined EXAFS and Raman data[44] for the tetrahedrally coordinated V═O terminal bond/stretching on alumina supported vanadia catalysts demonstrate that a terminal V═O Raman band at 1022 cm^{-1} corresponds to a very short V═O bond length of 1.58 Å. Wachs' correlation[38,43,45] indicates that the V−O bond length should be much shorter than the corresponding Mo/W−O bond lengths for the M−O (M = V, Mo, W) Raman bands with the same vibrational frequency. For example, the V−O, Mo−O, and W−O bond lengths are estimated to be 1.60, 1.69, 1.71 Å, respectively, for a Raman frequency at 1000 cm^{-1}. Likewise, the correlation shows that the V−O stretching should appear at a much lower frequency than the Mo/W−O stretching at the identical V/Mo/W−O bond length. For example, Raman bands for the V−O, Mo−O, and W−O stretching are estimated to appear at 902, 1076, and 1120 cm^{-1}, respectively, at a single M−O bond length of 1.65 Å.

The difference in bond length/strength between V−O and Mo/W−O bonds is primarily due to the difference in valence. To satisfy the bond valence, a tetrahedrally coordinated

(40) Kolitsch, U. *Z. Kristallogr.* **2001**, *216*, 449−454.
(41) Amdouni, N.; Zarrouk, H.; Soulette, F.; Julien, C. M. *J. Mater. Chem.* **2003**, *13*, 2374−2380.
(42) Mestl, G.; Ruiz, P.; Delmon, B.; Knozinger, H. *J. Phys. Chem.* **1994**, *98*, 11269−11275.
(43) Hardcastle, F. D.; Wachs, I. E. *J. Phys. Chem.* **1991**, *95*, 5031−5041.
(44) Keller, D. E.; de Groot, F. M. F.; Koningsberger, D. C.; Weckhuysen, B. M. *J. Phys. Chem. B* **2005**, *109*, 10223−10233.
(45) Hardcastle, F. D.; Wachs, I. E. *J. Raman Spectrosc.* **1995**, *26*, 397−405.

VO_4^{3-} unit should have three 'single' bonds and one 'double' bond, while tetrahedrally coordinated MoO_4^{2-} or WO_4^{2-} units should have two 'single' bonds and two 'double' bonds. Therefore, the Mo/W−O bond orders tend to be higher than the corresponding V−O bond order for the same tetrahedral geometry. For example, a Mo═O double bond was observed by Raman spectroscopy in the mixed V/MoO_4 tetrahedra of $FeVMoO_7$ and $CrVMoO_7$. However, no vanadium−oxo double bond was observed even though the shortest V−O bond length of 1.65−1.66 Å is shorter than the shortest Mo−O bond length of 1.69 Å in the tetrahedral structure.[46]

Using 1.66 Å as an estimation for the V(1)−O(2) bond length associated with cation vacancies, a shoulder band appearing at 944 cm^{-1}, closest to the estimated frequency of 929 cm^{-1}, in the Raman spectrum of $Mg_{2.5}VMoO_8$ is assigned to the V(1)−O(2) stretching vibration. Supporting evidence is that the band at 944 cm^{-1} observed as a shoulder in the Raman spectrum of $Mg_{2.5}VMoO_8$ is not seen in the Raman spectrum of vacancy-filled and vanadium-missing $Li_2Mg_2(MoO_4)_3$. However, the shoulder is very weak, suggesting that the concentration of V(1)−O(2) bonds surrounding the vacancies are much less than the corresponding Mo(1)−O(2) bonds, and thus MoO_4 preferentially associates with the cation vacancies. If this V(1)−O(2) bond length is somewhat longer than ∼1.66 Å, then the vibrational assignment should be revised to the Raman band at 860 cm^{-1}, which shows similar spectral variation (red-shifted and weaker as x increases) to the band at 1016 cm^{-1}. The observed Raman frequencies and their assignments, as we understand them at the present time, are summarized in Table 2.

Because there is no definitive evidence of vanadium−oxo double bonds in the structure of $Mg_{2.5}VMoO_8$, short-range ordering may place predominately the molybdenum-centered tetrahedra nearest the cation vacancies. No long-range ordering of either the cation vacancies or the V/Mo tetrahedra has been observed by X-ray[13] or neutron diffraction,[25] but the relatively large thermal parameters associated with Mg(2) along the a axis have been attributed to the displacement of Mg^{2+} cations toward cation vacancies arising from columbic repulsions between the face-sharing Mg^{2+} cations.[13] The Mg(2) site is in the hexagonal tunnel on the 4c position, and one-fourth of these sites are empty on average. Clusters of trimers of face-sharing Mg^{2+} cations bordered by vacancies effectively relax the two Mg^{2+} cations at the end of the trimer which displace toward the vacancies. Such clusters may also couple to additional order of the tetrahedral sites that comprise the wall of the hexagonal tunnel. Specifically, the vacancies are surrounded by six Mo^{6+} centered tetrahedra. The two Mg^{2+} ions on the end of the trimer are surrounded by three V^{5+}- and three Mo^{6+}-centered tetrahedra, while the Mg^{2+} in the center of the trimer is surrounded by six V^{5+}-centered tetrahedra. The model is further illustrated in Figure 2b.

(46) Wang, X.; Heier, K. R.; Stern, C. L.; Poeppelmeier, K. R. *Inorg. Chem.* **1998**, *37*, 3252−3256.

Conclusions

A complete solid solution between the phases $Mg_{2.5}VMoO_8$ and $Li_2Mg_2(MoO_4)_3$ governed by the formula $\square_{1/4-x/6}Li_{4x/3}Mg_{15/4-7x/6}V_{3/2-x}Mo_{3/2+x}O_{12}$ ($0 \le x \le 1.5$) was discovered in which remarkably complex solid-state chemistry can be described by one variable. Cation vacancies are required to maintain electrical neutrality. High-frequency Mo═O Raman bands shift to lower frequencies, correlating with a decrease in the molybdenum−oxygen bonding, as the cation vacancies are filled. The apparent absence of V═O bands suggest local ordering of the VO_4 and MoO_4 tetrahedra surrounding the vacancies that places primarily MoO_4 tetrahedra around the cation vacancies.

Acknowledgment. The authors gratefully acknowledge the National Science Foundation, Solid State Chemistry (Award Nos. DMR-9727516 and DMR-0312136), the EMSI program of the National Science Foundation at the Northwestern University Institute for Environmental Catalysis (Grant No. 9810378), and the Department of Energy, BES-Chemical Sciences, Geosciences, and Biosciences Division under Grant No. DE-FG0203ER15457 for support of this work. The authors made use of the Central Facilities supported by the MRSEC program of the National Science Foundation (Grant DMR-0076097) at the Materials Research Center of Northwestern University.

Note Added after ASAP Publication. This article was released ASAP on December 27, 2005, with arrows missing in Table 2. The correct version was published on January 6, 2006.

IC051741+